Observation of ultrathin metastable fcc Ti films on Al(110) surfaces

Adli A. Saleh, V. Shutthanandan, and R. J. Smith
Physics Department, Montana State University, Bozeman, Montana 59717
(Received 8 March 1993; revised manuscript received 2 September 1993)

High-energy ion-scattering spectroscopy, x-ray-photoemission spectroscopy, and low-energy electron diffraction (LEED) were used to study the growth of very thin Ti films on Al(110) surfaces at room temperature. The Al surface peak areas in the backscattering spectra of 0.96-MeV He^+ ions, incident along the $[\bar{1}\,\bar{1}0]$ direction of Al(110), decreased sharply during the deposition of the first five monolayers of Ti. This suggests a growth model in which a pseudomorphic Ti film with a fcc structure forms, shadowing the Al surface atoms. This model is supported by LEED measurements where sharp diffraction spots persisted with the rectangular symmetry of the substrate lattice structure. Throughout this coverage regime, the attenuation of the Al photopeak intensities as a function of Ti coverage agrees with the attenuation rate calculated using a laminar growth mode. With additional Ti deposition the Al surface peak intensities increase while the Al photopeak intensities remain unchanged. A discussion of possible growth models for the high-coverage regime is presented.

INTRODUCTION

Epitaxial growth of ultrathin metallic films on single-crystal substrates in an ultrahigh-vacuum (UHV) environment continues to receive a considerable amount of attention. These systems exhibit interesting physical properties and are important in the search for new materials. The interfacial strain associated with the misfit between the substrate and overlayer lattice structures, as well as the difference in the surface free energy between the overlayer and the substrate materials, circumscribe the structures formed. The modified electronic and geometric structures in the overlayer may result in different physical properties for the deposited film as compared to those of the bulk material. Palladium, for example, shows an enhanced magnetic susceptibility associated with the expansion of the Pd unit cell in the Au-Pd-Au epitaxial structure.[1] Also, thin Pd films on Mo(100) exhibit a reduced hydrogen uptake relative to that for bulk Pd.[2] An interesting subgroup of these bilayer systems is one in which metastable overlayer phases form due to the adatom-substrate interaction. In these systems, new phases, or phases that exist only at elevated temperatures are stabilized on the substrate surface at room temperature. For example, face-centered cubic (fcc) Co films grow epitaxially on Cu(001) substrates, and body-centered cubic (bcc) Co films can be grown on Fe(001) thin films, whereas bulk Co exhibits a hexagonal close-packed (hcp) structure at room temperature.[3,4] A fcc Co film of up to 30 monolayers in thickness was observed to grow epitaxially on a Ni(001) surface.[5] These structures were identified primarily by means of the electron forward focusing associated with angle-resolved x-ray-photoemission and Auger-electron spectroscopies.[6]

In this study we report the growth of thin metastable Ti films with a fcc structure on Al(110) surfaces. High-energy ion scattering (HEIS) was used to characterize the film structure and thickness during the growth process. X-ray-photoemission spectroscopy (XPS) and low-energy electron diffraction (LEED) were also used to characterize the surface. The fcc Ti films grow to a thickness of about 5 ML. With additional Ti deposition, both the HEIS and the XPS measurements indicate an abrupt change in the film growth characteristics as the overlayer morphology changes and/or Ti-Al interdiffusion begins.

EXPERIMENTAL TECHNIQUES

High-energy ion scattering, when used in the channeling mode, provides a powerful tool to probe the substrate surface structure, as well as overlayer structures and growth modes.[7] In addition, HEIS provides a direct means for accurately measuring the overlayer coverage when the ion beam is incident on the substrate in a random direction. In the channeling geometry, the ion beam is incident along a low-index crystallographic direction, and the energy spectrum of backscattered particles exhibits a surface peak (SP) associated with ions backscattered from the topmost layers of the solid. The SP areas are converted to areal densities of visible target atoms (atoms/cm^2) by using the Rutherford-scattering cross section, the solid angle subtended by the detector, and the time-integrated incident ion flux. To extract information about the surface structure from the data, the experimentally measured ion yields are compared with the scattering yields calculated using computer simulations of the channeling measurements for various overlayer-substrate structures, as described below. LEED is used to supplement the short-range structural information, provided by HEIS with information about the degree of long-range order at the surface of the overlayer. Changes in pattern symmetries and diffraction-spot profiles can be attributed to structural modifications in the overlayer during the growth process. In the XPS experiments, the attenuation of the Al photopeak intensities as a function of Ti coverage is used to characterize the morphology of the Ti films. In addition, XPS is used to determine the

amount of contamination on the sample surface during the cleaning process.

The Al single crystals were cut and polished to within 0.5° of the (110) crystallographic plane, as measured using the Laue x-ray method.[8] Before being mounted in the UHV system, the samples were chemically etched for 15 seconds in an aqueous solution containing HCl(1.5%), HF(1.5%), and HNO_3(2.5%). High-purity Ti wires (99.99%), 0.25 mm in diameter, were wound into small filaments and then etched in a 20% HF solution. To deposit Ti on the Al surface, these filaments were resistively heated using a constant-current power supply to maintain a constant Ti sublimation rate. The Ti filaments were mounted 5″ away from the Al sample so that a uniform Ti flux was obtained across the sample surface. A deposition rate of about 0.5 monolayer/min, as measured by ion scattering, was obtained by maintaining a current of 4.5 A through the Ti wire. All Ti depositions were performed with the Al sample at room temperature.

The UHV chamber used for the HEIS measurements is connected to a 2-MV Van de Graaff accelerator through a differentially pumped beamline. The Al sample was mounted in the chamber on a thick Mo block which is attached to a three-axis goniometer for channeling measurements. The temperature of the Mo block was monitored using a calibrated Pt resistor mounted inside the block. After baking the UHV system, a pressure of 1.0×10^{-10} Torr was obtained. All filaments in the chamber were extensively outgassed during and after the system bakeout. A residual-gas analyzer was used to monitor the various gas components in the chamber. During the ion-scattering measurements the pressure in the chamber rose to about 5.0×10^{-10} Torr primarily due to the He^+ ion beam. Energy analysis of the backscattered particles for HEIS was performed using a bakable, passivated, implanted planar silicon (PIPS) detector installed on a rotatable arm and located 3″ away from the sample. The detector position was set at a scattering angle of 105° for these experiments. The UHV system also included an XPS capability that was used to verify the cleanliness of the Al surface. A more detailed description of the experimental setup has been published elsewhere.[9]

The samples were cleaned by repeated cycles of Ar^+ ion bombardment (1.5 keV) for several hours at a time, with the sample at room temperature, followed by annealing of the sample at 450 °C for 15 min. The photoemission spectrum for the sample, before cleaning, exhibited an Al $2p$ photopeak with a second component, at higher binding energy, that is associated with Al oxide (Al_2O_3). The cleaning procedure was repeated until the photopeak associated with the oxide was completely removed from the spectrum. The O $1s$ photopeak could not be used to monitor the Al surface oxide because the XPS analysis area included a small portion of the Mo sample holder surrounding the Al crystal. After the cleaning procedure was completed, a collimated beam of 0.96-MeV He^+ ions, passing through an aperture of 1.2 mm^2 in area, was used to carry out the ion-scattering measurements. The sample was aligned with the ion beam incident along the $[\bar{1}\,\bar{1}0]$ direction by minimizing the backscattered ion yield in a small region behind the surface peak. This procedure was repeated in an iterative manner using both the rotation and tilt angles of the sample goniometer. In a preliminary experiment to measure the damage induced by the incident He^+ beam, no appreciable increase in ion yield was observed after an ion dose of 3.1×10^{16} ions/cm^2. This result established the validity of the ion-scattering technique to carry out this surface study. Ion-scattering and XPS measurements were made after each Ti deposition. A total dose of 1.56×10^{15} ions/cm^2 was used to collect each HEIS spectrum. In addition, an ion-scattering spectrum was measured, but less frequently, with the sample rotated out of the channeling alignment to determine the total Ti coverage at the different stages of the experiment. These measurements in a random-alignment geometry eliminate possible errors, associated with the shadowing of Ti atoms, in determining the Ti coverage.

A second set of Ti deposition experiments was performed in a different UHV system in which XPS and LEED measurements were done. The XPS data were taken using a Mg $K\alpha$ source ($h\nu=1253.6$ eV). Emitted photoelectrons were collected and analyzed using a hemispherical analyzer in the fixed-transmission mode with an energy resolution of 1.0 eV, as determined from the width of the $3d$ photopeaks using a standard Ag foil. The sputter-annealing procedure described above was again used for cleaning the sample. The LEED measurements were carried out using Varian optics with the electron beam incident normal to the sample surface. A $p(1\times1)$ pattern was obtained after annealing the sample and served as evidence for an ordered Al surface. X-ray-photoelectron spectra for the Al $2p$ and Al $2s$ photopeaks were recorded after each Ti deposition. The inelastic mean free path (IMFP) for these photoelectrons, with a kinetic energy of around 1400 eV, is about 20 Å.[10] The amount of each Ti deposition was monitored using a quartz-crystal oscillator (QCO) which was water cooled to maintain thermal stability during deposition. After the last deposition, the Al sample, with the deposited Ti film, was mounted in another vacuum chamber, equipped for Rutherford-backscattering spectroscopy, to determine the total Ti coverage on the Al sample, and thus calibrate the QCO measurements.

RESULTS

Figure 1 shows two ion-scattering spectra collected after sputter-cleaning and annealing the sample. One spectrum (○) was taken with the ion beam incident on the sample in a near-normal, random direction, while the other spectrum (●) was taken with the beam incident along the $[\bar{1}\,\bar{1}0]$ direction, i.e., normal incidence. For random incidence, the measured spectrum height agrees with the theoretically calculated height[7] using tabulated values for the stopping power of He ions in Al.[11] The measured value for the normalized, minimum yield χ_{min} was 4.0%. The calculated value for χ_{min} is 3.7%, using a one-dimensional thermal-vibration amplitude of 0.105 Å and a crystal lattice constant of 4.05 Å.[12] This good agreement is important since it serves as a measure of crystal quality. Larger measured values of χ_{min} might in-

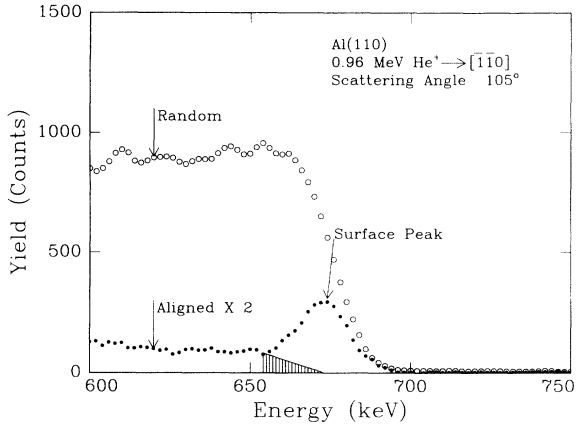

FIG. 1. He^+ ion scattering spectra at 0.96-MeV incident ion energy for a clean Al(110) surface. ○: spectrum taken at random incidence; ●: spectrum for incidence along the [1̄ 1̄0] direction. The shaded triangle represents the subtracted background when peak areas are converted to hitting probabilities.

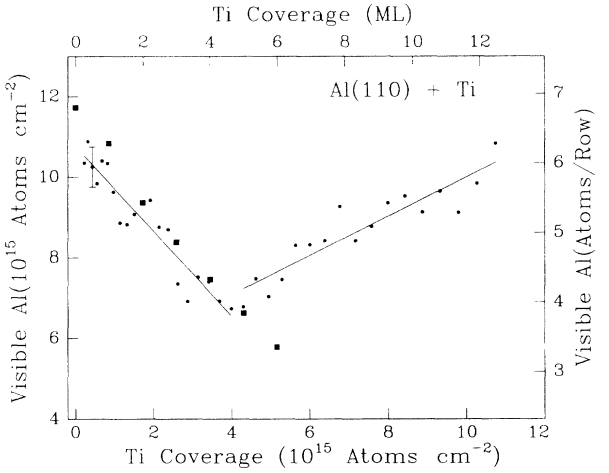

FIG. 2. Visible Al atoms, at 0.96-MeV incident ion energy, as a function of Ti coverage deposited at room temperature on Al(110). The error bar represents an uncertainty of ±5% in the measurement of SP areas. Two regions are indicated. The solid lines are linear fits to the data, intended to guide the eye. The ■ indicate the expected yield for a flat, pseudomorphic Ti film as calculated using the VEGAS simulation code.

dicate, for example, the presence of deeply embedded transition-metal atoms remaining from earlier experiments, or defects associated with sputtering and sample preparation, all of which could result in increased ion dechanneling. The measured SP area in the aligned spectrum corresponds to 6.8 atoms/row. This value agrees quite well with the theoretical value of 6.9 atoms/row that is obtained by simulating the scattering of He^+ ions from a clean Al(110) surface. This computer simulation was carried out using the VEGAS code which uses Monte Carlo calculations and a Moliere screened potential.[13] A thermal-vibration amplitude of 0.105 Å and the known multilayer relaxation of the Al(110) surface were the input parameters in the simulation.[14] The areas of the surface peaks due to Al were determined using the triangular background subtraction method.[15] In this method, the area of the shaded triangle, shown in Fig. 1 and defined by the channel numbers of the SP centroid and the minimum yield, is subtracted from the total peak area.

In Fig. 2, we plot the number of Al atoms/cm^2 visible to the incident ion beam as a function of Ti coverage. The Al(110) surface density of 0.86×10^{15} atoms/cm^2 per monolayer was used to convert the Ti coverage into equivalent Al(110) monolayers. The scatter in the Al SP areas is associated more with the background subtraction procedure than with the reproducibility of the spectra. The Al SP area initially decreases with Ti deposition, indicating a lower Al hitting probability. This decrease is attributed to shadowing of the surface Al atoms by Ti atoms. As more Ti is deposited on the substrate, exceeding the critical thickness of about 5 ML, the initial growth regime is followed by one in which the number of substrate atoms exposed to the incident ion beam increases, as shown by the increase in the Al SP areas in Fig. 2. This increase continues up to a total coverage of 12.5 ML of Ti, at which coverage the experiment was terminated.

A comparison between the HEIS spectra collected for aligned and random ion incidence reveals a slightly smaller Ti SP area in the aligned geometry, as shown in Fig. 3. This small, but measurable, difference in the Ti hitting probability indicates that the overlayer has some degree of axial alignment with respect to the Al substrate. A plot of the number of Ti atoms visible to the incident ion beam in the aligned geometry versus the Ti coverage, as measured with a random incident direction, is shown in Fig. 4. Negligible Ti shadowing was observed for Ti coverages less than 4 ML.

The LEED and XPS results from our second experiment are shown in Figs. 5 and 6, respectively. After sputter-cleaning and annealing the surface, sharp LEED

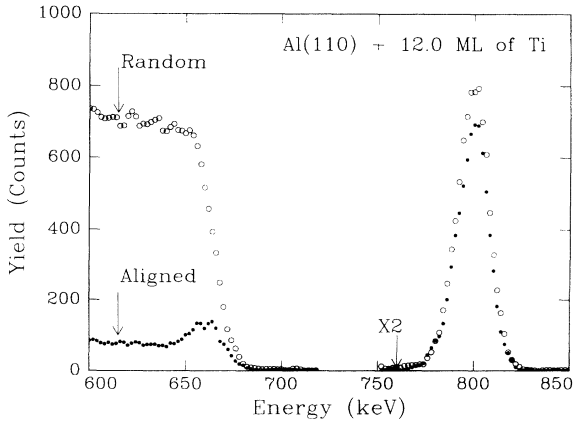

FIG. 3. He^+ ion scattering spectra at 0.96-MeV incident ion energy after the deposition of 12.0 ML of Ti. ○: spectrum taken at random incidence; ●: spectrum for incidence along the [1̄ 1̄0] direction. That portion of the spectrum which shows the Ti peaks has been enlarged by a factor of 2.

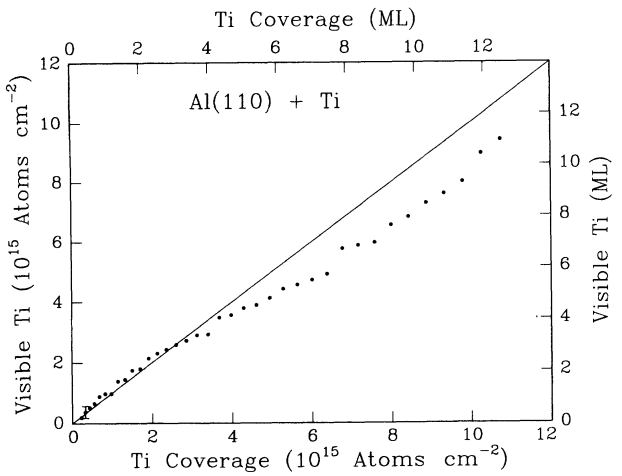

FIG. 4. Visible Ti atoms, at 0.96-MeV incident ion energy, as a function of Ti overlayer coverage. Evidence for Ti shadowing is observed for coverages greater than 4 ML. The solid line shows the yield measured for a random overlayer.

spots in a rectangular pattern were obtained, reflecting the (110) surface symmetry, and also supporting the cleanliness of the Al surface. The low electron-beam kinetic energy of 42.0 eV facilitated probing the structure of the topmost surface layers. Pictures of the LEED spots are shown in Figs. 5(a)–5(d) for the clean surface, and for Ti coverages of 1.4, 2.8, and 5.5 ML, respectively. Ti deposition did not induce noticeable changes in the LEED pattern up to a coverage of about 5 ML, at which point the spots broadened and became less intense, as shown in Fig. 5(d). These results are consistent with the initial formation of a pseudomorphic Ti film, followed by some form of nonlaminar, or disordered, growth as discussed below.

The variation in the photoemission intensities can be used to further understand the structure of the overlayer. Peak areas for the Al 2*p* photopeak were obtained by subtracting a straight baseline background from the original data. A plot of the Al 2*p* photopeak area as a function of Ti coverage is shown in Fig. 6. The initial decrease in the photoemission intensity is associated with the formation of a Ti film with uniform thickness. The intensity of the Al 2*p* photoelectrons decreased to about 40% of the original value after the deposition of 3 ML of Ti. The intensity variation levels off at higher Ti coverages, indicating a change in the character of the overlayer growth mode with additional Ti deposition. This measurement of the critical thickness for the overlayer is smaller than, but in reasonable agreement with, our estimate based on channeling measurements. The variation in the Al 2*s* XPS peak area as a function of Ti coverage shows the same trends as observed for the Al 2*p* photopeak.

DISCUSSION OF RESULTS

As shown in Fig. 2, there appear to be two distinct growth regimes for these ultrathin films of Ti on Al(110), corresponding to Ti coverages of less than, and greater than, 5 ML. The main point of this paper is that in the

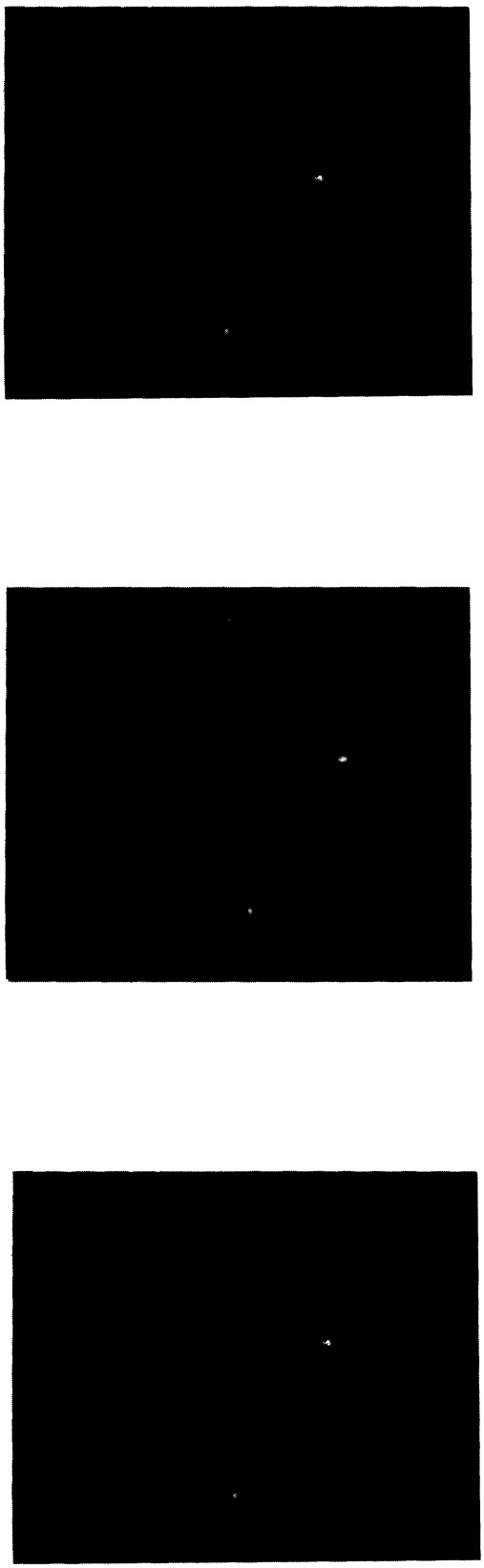

FIG. 5. LEED patterns for Al(110)+Ti at 42.0 eV. The [1$\bar{1}$0] direction is up in the figure. The spots are the (01), (10), and (0$\bar{1}$), clockwise from the top of the figures. The patterns are for (a) clean Al, and for Ti coverages of (b) 1.4 ML, (c) 2.8 ML and (d) 5.5 ML.

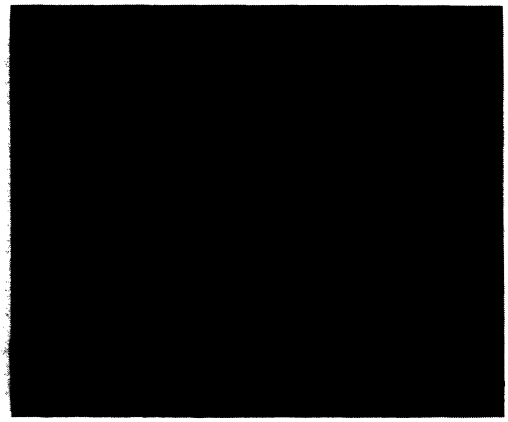

FIG. 5. (*Continued*).

low-coverage regime a flat, pseudomorphic film of *fcc* Ti grows to a critical thickness of approximately 5 monolayers. This is particularly interesting because, while bulk Ti assumes a hcp structure at room temperature, and transforms to a bcc structure above 877 °C, the fcc structure does not occur in the equilibrium phase diagram of Ti at any temperature.[16] Thus, the thin, fcc Ti film is in a metastable condition, confined by the Ti-Al bonding at the interface. A critical thickness is reached, at a Ti coverage of approximately 5 ML, when the strain energy in the film exceeds the interfacial energy, and a modification of the film structure occurs. These conclusions are based on the following considerations.

The observations for low Ti coverages include the following: the Al surface peak area is attenuated as a function of Ti coverage (Fig. 2), the intensity of the Al photopeak is also attenuated with increasing Ti coverage (Fig. 6), and the LEED spots remain sharp and exhibit the rectangular symmetry of the substrate [Figs. 5(a)–5(c)]. The initial decrease in the SP area associated with the Al substrate atoms is attributed to the formation of a pseudomorphic overlayer in which Ti atoms adopt the surface symmetry and lattice constant of the substrate, and thus shadow the underlying Al atoms. This decrease continues for Ti coverages up to about 5 ML, when the Al hitting probability reaches a minimum of 3.9 atoms/row. A linear fit to these data yields a slope of -0.96 Al atoms per Ti atom, indicating the equivalent shadowing of about one Al atom for every deposited Ti atom. We compared this dependence on Ti coverage to that obtained from computer simulations of the experiment, using the VEGAS code.[13] In these simulations, the Ti atoms were placed on Al lattice sites above the surface, in a layer-by-layer fashion, with the Al(110) interplanar distance, 1.432 Å. The vibration amplitude for Ti atoms was assumed to be the same as that for Al atoms, namely, 0.105 Å. This is a reasonable approximation since the Debye temperature of Ti (380 K) is close to that for Al (394 K).[8] The results of these simulations at various Ti coverages below the critical thickness are in excellent agreement with the measured yields, as indicated by the ■ symbols in Fig. 2. A slope of -1.05 Al atom per Ti atom is obtained from a linear fit applied to the results of the computer simulations.

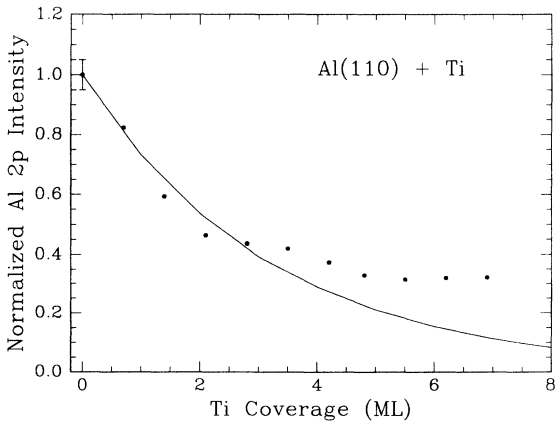

FIG. 6. Normalized Al $2p$ photoelectron intensities plotted as a function of Ti coverage on the Al(110) surface. The solid line is the theoretical calculation for a layer-by-layer growth mode, using an inelastic mean free path of 4.6 Å, as discussed in the text. The error bar represents the uncertainty in peak area associated with our background subtraction procedure.

Our results for Al shadowing as a function of Ti coverage indicate not only that the Ti film is pseudomorphic, but also that it is relatively flat. If any portion of the overlayer were redistributed to form Ti islands, the simulations indicate that there would be less shadowing of the Al atoms than is observed, and measurable shadowing of Ti atoms. For example, the simulations show that Ti-Ti shadowing for a coverage of 4 ML (2 atoms/row) is only 0.05 atoms/row, which is less than our experimental error of about 0.2 atoms/row. However, for a film thickness of 3 atoms/row (6 ML) the calculated Ti-Ti shadowing is 0.23 atoms/row. Thus, for 2 ML of Ti coverage, any redistribution of the Ti atoms to form pseudomorphic islands would lead to a thickness ≥ 3.0 atoms/row in some regions of the surface, and would result in measurable Ti shadowing. At a Ti coverage of 4 ML, no shadowing of Ti was observed, as shown in Fig. 4. The measured shadowing of Al atoms corresponds to the maximum value that can be obtained at a given coverage, using the coordinates of the Al lattice and our ion energy, and thus supports the model of a flat, pseudomorphic film. The persistence of the LEED spots with the substrate symmetry, as shown in Fig. 5, lends additional support to this model. We also considered the possibility that various orientations of distorted bcc or hcp Ti overlayers were growing on the surface for low Ti coverages, but found that every configuration considered could be eliminated based on the lack of agreement with the ion-scattering results for Al shadowing.

The attenuation of the Al photopeak intensity at low Ti coverages, shown in Fig. 6, further supports a model of flat, pseudomorphic film growth. The solid line in Fig. 6 shows the variation expected for the Al $2p$ photopeak intensity using an ideal, layer-by-layer growth mode. The attenuation of the intensity after the completion of h monolayers, plus an additional partial coverage x of the topmost layer, is described by $I_{\mathrm{Al}}(h,x)=w^h(1-x+xw)$.[17] Here, I_{Al} is the Al photopeak intensity, nor-

malized to the intensity for the clean Al substrate; w is an attenuation factor expressed as $\exp[-d/(\lambda\cos\theta)]$, where d and λ are the interplanar distance in the overlayer and the inelastic mean free path (IMFP) for inelastic scattering of electrons, respectively; θ is the photoelectron exit angle relative to the surface normal (0° in this case). An important point in such models of emission intensity is that a flat film gives the greatest possible attenuation of the substrate photopeak intensity. Any combination of layers and islands, i.e., a nonuniform thickness, will lead to a larger intensity than that calculated for laminar growth.[18] There is some ambiguity, however, in applying this model for emission intensity, since the IMFP is not always known. The value for λ obtained from the universal curve can be considerably larger than the value obtained in experiments for very thin epitaxial films.[3] Furthermore, when diffraction effects are present, the rate of attenuation is strongly dependent on the emission angle, which can lead to an overestimation of λ.[19] Thus, we took the ion-scattering data as strong evidence for the initial growth of a flat film. We then assumed a layer-by-layer growth model for the Al photopeak intensity, and adjusted λ for the best fit to the XPS data of Fig. 6 at Ti coverages below 4 ML. The resulting value for λ was 4.6 Å, considerably smaller than the value of 20 Å obtained from the universal curve. Larger values of λ would result in less rapid attenuation of the Al emission intensity at low Ti coverages.

While there is little doubt about the structure and morphology of the Ti film at low Ti coverages, the situation at coverages greater than 5 ML is not so clear. The observations are (1) shadowing of Al atoms gradually decreases, (2) shadowing of Ti atoms is observed, (3) the LEED spots broaden and their intensity decreases, and (4) the Al photopeak intensity decreases at a slower rate. Some possible transformations of the film, and the corresponding driving mechanisms, include the introduction of misfit dislocations, which reduces the accumulated strain in the overlayer; the formation of islands by surface diffusion, which lowers the surface free energy; and the interdiffusion of Ti and Al atoms at the interface, which lowers the total energy through the release of the Ti-Al formation energy. We note that the surface free energy for Al, 1.085 J/m^2, is considerably smaller than that for Ti, 2.570 J/m^2.[20] The difference in these values puts a lower limit on the interface energy associated with Ti-Al bonding and film stress. Of the three possibilities just mentioned, the formation of islands would account for all of our observations for Ti coverages above 5 ML. Island formation would result in broad, diffuse LEED spots as seen in Fig. 5(d). Island formation would also result in increased Ti-Ti shadowing, and the gradual exposure of previously shadowed Al atoms to the incident ion beam. Finally, the XPS intensity rises above the layer-by-layer model calculation, consistent with island formation. Although the islands may still be pseudomorphic with the substrate lattice, the onset of misfit dislocations is quite likely.

Interdiffusion of Ti and Al atoms at the interface is also possible. We note that the formation energy for most observed Ti-Al compounds is negative, ranging from −25 to −38 kJ/mole.[21] These values are only slightly smaller than typical values for the formation energy of Ni-Al, where considerable interface reaction is observed.[22] Furthermore, while the solubility of Ti in Al is negligible at room temperature, there is a limited solubility of Al in Ti.[16] Thus, out-diffusion of the substrate atoms might begin when some critical thickness is achieved in the overlayer, and defects are introduced into the film. Diffusion of Al atoms into the overlayer could also explain the XPS results seen at higher coverages in Fig. 6, and, depending on the degree of order, could result in the shadowing of Ti atoms by Al atoms in the overlayer. We do observe considerable interdiffusion when the Ti/Al(110) bilayer is heated above 450 °C.[23] Thus, we conclude that a combination of diffusion and island formation may be occurring for Ti coverages greater than 5 ML.

A final point can be made about the critical thickness at which the pseudomorphic Ti film undergoes a transformation. We make use of an expression derived by Jesser and Kuhlmann-Wilsdorf,[24] based on the earlier work of van der Merwe,[25] which predicts the critical thickness at which the energy in the strained, pseudomorphic overlayer just equals the interface energy associated with a particular lattice mismatch. Using the elastic constants of Ti and Al,[26] we obtain a lattice mismatch of 4.4% for a critical thickness of 5 ML. This mismatch corresponds to an interatomic distance of 2.99 Å, as compared to the nearest-neighbor distance of 2.86 Å in Al. The value of 2.99 Å is very close to the nearest-neighbor distance for Ti in the hexagonal structure (2.95 Å). We do not know the interatomic distance for fcc Ti since it does not exist in nature, but the behavior of Co may serve as a guide. Cobalt assumes the hexagonal structure at room temperature, with a nearest-neighbor distance of 2.507 Å, and transforms to the fcc structure, with an interatomic distance of 2.506 Å, at elevated temperatures.[27] This is reasonable since the main difference between these two structures is the stacking sequence for the close-packed planes. Thus, it is reasonable to assume that fcc Ti has approximately the same interatomic distance as the room-temperature hexagonal phase, resulting in the measured critical thickness of about 5 ML, and in excellent agreement with the predictions of the continuum theory. An interatomic distance of 2.95 Å corresponds to a critical thickness of 5.5 ML. The agreement here may be fortuitous since the application of the continuum model to these ultrathin, epitaxial films may be suspect when the film thickness is comparable to the dislocation core radius.[28]

We also considered other Ti structures as candidates for the pseudomorphic overlayer. The lattice mismatch for bcc Ti is too large, about 16% along [100]. The hcp Ti structure has the appropriate interatomic distance but does not lead to the observed shadowing of Al atoms. γ-TiAl has a face-centered tetragonal structure that closely matches the Al lattice, with a 2% lattice mismatch,[16] but again cannot account for the Al shadowing results up to 5 ML of Ti coverage. The formation of titanium hydrides on Al(110) was also considered as a possibility in the initial growth stage because Ti has a strong affinity

for H. The γ-hydride phase, with a H/Ti atomic ratio of 1.5 or greater, has a face-centered cubic fluorite structure, and a lattice misfit of about 10% with respect to the Al substrate.[29] However, we believe that the hydrogen concentration in our Ti films was less than one monolayer, based on experiments in progress on the Al(100) surface.[23] For Al(100) we also observe pseudomorphic growth of Ti up to 5 ML, with shadowing behavior very similar to that shown for Al(110) in Fig. 2. Forward-scattering, elastic-recoil measurements[30] (ERDA) were made to determine the total concentration of hydrogen in the Ti films. The measured concentration of hydrogen in a 5-ML Ti film was negligible. Even our thicker films on Al(100) showed little more than a monolayer of chemisorbed hydrogen at the end of the experiments. Thus, we believe that hydride formation is not occurring for these Ti films on Al(110). We plan to use ERDA to characterize the hydrogen absorption of the Ti films on Al(110) in future experiments.

In summary, we conclude that a flat, pseudomorphic Ti film forms initially for Ti deposition on the Al(110) substrate. Up to a critical trickiness of 5 ML, the Ti/Al interface is abrupt, and no evidence for displacement of Al atoms is observed. For coverages greater than 5 ML, an undetermined combination of island formation and Ti-Al interdiffusion occurs, leading to increased visibility of the Al atoms in ion-scattering measurements. The critical thickness of 5 ML is found to be in excellent agreement with the interatomic distance expected for fcc Ti, using a continuum model for epitaxial film growth.

ACKNOWLEDGMENTS

The authors would like to thank Dr. James Anderson for his assistance in the LEED and XPS measurements. This work was supported by the Montana Space Grant Consortium, NASA Grant No. GT40041, and NSF EPSCOR No. RII-89211978 (MONTS).

[1]M. B. Brodsky and A. J. Freeman, Phys. Rev. Lett. **45**, 133 (1980).
[2]J. M. Heitzinger, S. C. Gebhard, and B. E. Koel, Chem. Phys. Lett. **200**, 65 (1992).
[3]Hong Li and B. P. Tonner, Surf. Sci. **237**, 141 (1990).
[4]Hong Li and B. P. Tonner, Phys. Rev. B **40**, 10 241 (1989).
[5]S. A. Chambers, S. B. Anderson, H.-W. Chen, and J. H. Weaver, Phys. Rev. B **35**, 2592 (1987).
[6]S. A. Chambers, Adv. Phys. **40**, 357 (1991).
[7]L. C. Feldman, J. W. Mayer, and S. T. Picraux, *Materials Analysis by Ion Channeling* (Academic, New York, 1982).
[8]N. W. Ashcroft and N. David Mermin, *Solid State Physics* (Holt, Rinehart and Winston, New York, 1976), p. 101.
[9]R. J. Smith, C. N. Whang, Xu Mingde, M. Worthington, C. Hennessy, M. Kim, and N. Holland, Rev. Sci. Instrum. **58**, 2284 (1987).
[10]M. P. Seah and W. A. Dench, Surf. Anal. **1**, 2 (1979).
[11]J. F. Ziegler and W. K. Chu, At. Data Nucl. Data Tables **13**, 463 (1974).
[12]D. S. Gemmel, Rev. Mod. Phys. **46**, 129 (1974).
[13]J. W. Frenken, R. M. Tromp, and J. F. van der Veen, Nucl. Instrum. Methods B **17**, 334 (1986).
[14]R. J. Noonan and H. L. Davis, Phys. Rev. B **29**, 4349 (1984).
[15]I. Stensgaard, L. C. Feldman, and P. J. Silverman, Surf. Sci. **77**, 513 (1978).
[16]M. Hansen, *Constitution of Binary Alloys* (McGraw-Hill, New York, 1958), p. 139.
[17]Stefano Ossicini, Rossela Memeo, and Franco Ciccacci, J. Vac. Sci. Technol. A **3**, 387 (1985).
[18]L. C. Feldman and J. W. Mayer, *Fundamentals of Surface and Thin Film Analysis* (North-Holland, New York, 1986), p. 138.
[19]Y. U. Idzerda, D. M. Lind, and G. A. Prinz, J. Vac. Sci. Technol. A **7**, 1341 (1989).
[20]L. Z. Mezey and J. Giber, Jpn. J. Appl. Phys. **21**, 1569 (1982).
[21]F. R. de Boer, R. Boom, W. C. M. Mattens, A. R. Miedema, and A. K. Niessen, *Cohesion in Metals: Transition Metal Alloys* (North-Holland, Amsterdam, 1988).
[22]V. Shutthanandan, Adli A. Saleh, and R. J. Smith, J. Vac. Sci. Technol. A **11**, 1780 (1993).
[23]Adli Saleh, V. Shutthanandan, and R. J. Smith (unpublished).
[24]W. A. Jesser and D. Kuhlmann-Wilsdorf, Phys. Status Solidi **19**, 95 (1967).
[25]J. H. van der Merwe, J. Appl. Phys. **34**, 117 (1963); **34**, 123 (1963).
[26]*American Institute of Physics Handbook,* 2nd ed., edited by Dwight E. Gray (McGraw-Hil, New York, 1963).
[27]*Metals Handbook,* 8th ed., edited by Taylor Lyman (American Society for Metals, Metals Park, OH, 1964), Vol. 1, p. 1201.
[28]A. P. Payne, W. D. Nix, B. M. Lairson, and B. M. Clemens, Phys. Rev. B **47**, 13 730 (1993).
[29]H. Numakura and M. Koiwa, Acta Metall. **32**, 1799 (1984); William M. Mueller, James P. Blackledge, and George G. Libowitz, *Metal Hydrides* (Academic, New York, 1968), p. 352.
[30]A. Turos and O. Meyer, Nucl. Instrum. Methods B **4**, 92 (1984).

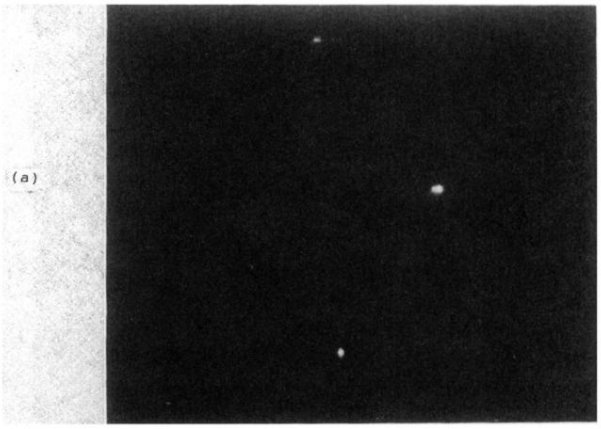

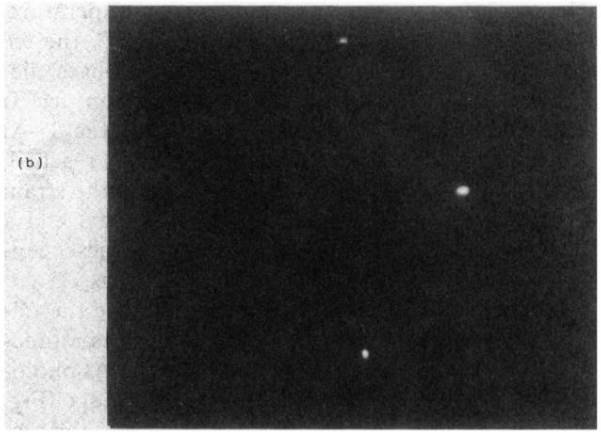

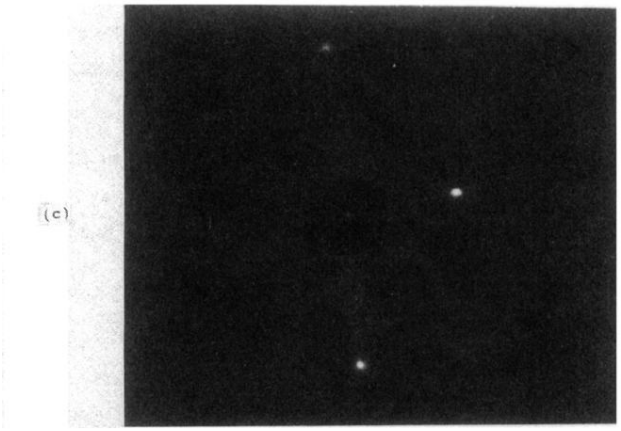

FIG. 5. LEED patterns for Al(110)+Ti at 42.0 eV. The $[1\bar{1}0]$ direction is up in the figure. The spots are the (01), (10), and $(0\bar{1})$, clockwise from the top of the figures. The patterns are for (a) clean Al, and for Ti coverages of (b) 1.4 ML, (c) 2.8 ML and (d) 5.5 ML.

(d)

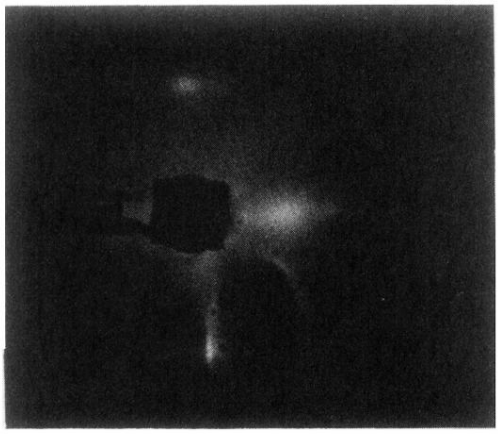

FIG. 5. (*Continued*).